DURABILITY-BASED DESIGN CRITERIA FOR A QUASI-ISOTROPIC CARBON FIBER AUTOMOTIVE COMPOSITE

J. M. Corum, R. L. Battiste, and M. B. Ruggles-Wrenn
Oak Ridge National Laboratory*
Oak Ridge, Tennessee 37831-8051

ABSTRACT

A major impediment to the increased application of composites for large structural automotive components is the lack of design guidelines to assure the required 15-year durability. This paper describes the development of durability-based design criteria for a quasi-isotropic carbon-fiber composite for possible automotive structural applications. The composite, which was made by a rapid-molding process suitable for high-volume automotive applications, consisted of continuous Thornel T300 fibers (6K tow) in a urea/urethane matrix. The reinforcement was in the form of four ±45E stitch-bonded mats in the following layup: $[0/90/\pm45]_S$. In addition to elastic and creep properties for design analyses, allowable time-dependent static stresses and allowable cyclic stresses are provided. Knockdown factors are incorporated to account for temperature effects and for the degrading effects of exposure to fluid environments. Stress state and, in the case of cyclic loadings, mean stress effects are also incorporated into the criteria.

KEY WORDS: Composite Materials, Durability, Design Criteria

1. INTRODUCTION

The widespread use of composite systems to produce large structural automotive components requires that their long-term durability be assured. An Oak Ridge National Laboratory (ORNL) project, sponsored by the U.S. Department of Energy and closely coordinated with the Automotive Composites Consortium (ACC) is charged with developing the means for providing this assurance. The approach is to develop experimentally based, durability-driven design criteria for representative carbon-fiber-based composite systems. Durability issues being examined include the potentially degrading effects of both sustained and cyclic loadings, exposure to automotive fluids, temperature extremes, and low-energy impacts (for example, from tool drops and kickups of roadway debris) and how they affect structural strength, stiffness, and dimensional stability.

---

*Oak Ridge National Laboratory, managed by UT-Battelle, LLC, for the U.S. Dept. of Energy under contract DE-AC05-00OR22725.

The project focus has been on the following progression of thermoset materials, all having the same urethane matrix:

- reference $[\pm 45]_{3S}$ crossply composite,
- $[0/90/\pm 45]_S$ quasi-isotropic composite, and
- chopped-fiber composite.

Characterization of the first two systems has been completed and reported (1,2). The resulting design criteria for the quasi-isotropic composite is the subject of this paper. The chopped-fiber composite is currently being characterized.

Both the crossply and the quasi-isotropic composites consisted of Thornel T300 continuous fibers (6K version) in a Baydur 420 IMR urethane matrix. The reinforcement was in the form of ±45E stitch-bonded mats. Six mats were used in the 3.2-mm-thick crossply composite plaques. Four mats were used in the quasi-isotropic composite, which was 2.2 mm thick. The fiber-volume content was approximately 40% in both cases.

The 610- by 610-mm plaques were molded by ACC using an "Injection-Compression Procedure." For this process a preform is produced by assembling the required layup of ±45° mats and introducing them into a mold. The mold is left open approximately 10-15-mm. The matrix is produced via the Structural Reaction Injection Molding (SRIM) process in which the two reactive systems, polyol and polymeric isocyanate, are pumped at high pressure into an impingement mixing chamber to quickly produce a uniform mixture of the components. The reacting mixture is then pumped into the partially open mold that contains the reinforcement, after which the mold is fully closed. This allows the resin to first flow, with little resistance, across the upper surface of the preform and then, under increasing closing pressure, flow through the thickness of the preform. This procedure results in less disturbance of the fiber orientation and produces a more uniform, void-free, distribution of resin through the carbon-fiber preform. The time required for the liquid-to-solid transformation is of the order of 15-20 s. Final postcure was 1 hour in a preheated oven at 130°C.

The average room temperature tensile properties of the quasi-isotropic composite are:

- ultimate tensile strength, 336 MPa,
- Young's Modulus, 32.4 GPa, and
- Failure ductility, 1.02%.

More than 1400 individual tests of laboratory specimens were performed to replicate on-road conditions and to generate data to form the basis for developing correlations and models for the quasi-isotopic composite. These correlations and models were then used to formulate design criteria. The types of tests included the following:

- basic short-time tension, compression, and shear;
- uniaxial and biaxial flexure;
- cyclic fatigue, including mean stress effects;
- tensile and compressive creep and creep rupture;
- tests of hole effects;*

- low-energy impact;[*] and
- compression-after-impact.[*]

In most cases, characterization of the effects of temperature and fluid exposure was included in the test effort. The specimen configurations and test methods were generally the same as those used previously to address the durability of glass-fiber composites (3).

Despite the relatively large number of tests performed, more extensive testing would be needed in several areas to provide sufficient data for developing completely defensible correlations, models, and design criteria. The approach taken here was to first perform as many carefully planned tests as possible within time and budget constraints. Then the design criteria were developed with the philosophy of providing the best possible engineering design guidance given the limited information available. This sometimes required assumptions and extrapolations beyond the range of the existing data. Clearly, while the information in this paper should be adequate for preliminary designs undertaken with this material and for comparative purposes with other materials, more information would likely be required for final design purposes.

For the design criteria, it was assumed that an automobile with a composite structure must last for 15 years (131,000 hours) and 150,000 miles. It was further assumed that during the 15 years, the vehicle will actually be operated about 5000 hours. The design temperature range was taken to vary from a minimum of –40°C to a maximum of 120°C, with the higher temperatures occurring only during operation.

In addition to functional stiffness and deformation requirements, structures must support and resist a variety of live and dead loads. During operation, for example, live loads might include a combination of pothole impact, hard turn, and maximum acceleration. Dead loads during the 15-year life would include those from the weight of the vehicle or sustained loads in the bed of a light truck.

Structures will also be exposed to common vehicle fluids and operating atmospheres, and design limits must take the resulting property degradation into account. The effects of a variety of fluids and moisture conditions were examined in the case of glass-fiber composites and in screening tests on the crossply carbon-fiber composite. Based on the combined finding, the fluids most extensively examined here were reduced primarily to distilled water and windshield washer fluid (a methanol/water mix).

The following three sections correspond to the three main parts of the design guidance: 1) material properties for design analyses, 2) time-dependent allowable stresses for static loads, and 3) design rules for cyclic loads. In each case, the supporting data are described and design guidance is provided.

[*] Information from these test types was used in formulating damage tolerance assessment guidelines, which are not covered in this paper.

2. ELASTIC AND CREEP PROPERTIES FOR DESIGN ANALYSES

It is presumed that design of automotive structural components will primarily employ linear-elastic finite-element plate and shell analyses, which are based on the material being homogeneous and isotropic. In addition to deformations, these analyses provide normal membrane and bending stresses plus shear in the relatively thin molded sections envisioned for automotive structures. Thus, elastic constants are required for analysis. Also, a means for at least approximately accounting for time-dependent creep is required. The necessary properties for doing this are presented in this section.

2.1 Elastic Constants It is shown in reference (2) that, except at higher temperatures and stresses, the quasi-isotropic composite is isotropic in the plane of the plaque.* For such an anisotropic layup that exhibits in-plane isotropy, the linear elastic response to in-plane applied loads is characterized by two constants, E and G, or alternatively, E and ν, where E and G are the Young's and shear moduli, and ν is Poisson's ratio. The constants are related by the following equation:

$$G = \frac{E}{2\left(1+\nu\right)} \quad . \qquad [1]$$

Elastic property data from tensile tests and Iosipescu shear tests on V-notch beams confirm that equation 1 is valid for the quasi-isotropic composite over the entire temperature range from –40° to 120°C.

Figure 1 shows the variation of Young's modulus with temperature. Measured Poisson's ratio values are also shown at specific temperatures.

Elastic properties are affected by prior cyclic loadings and, to a lesser extent, by exposure to fluids and to high humidity levels. These effects should be accounted for as appropriate. It was found that, repeated temperature cycling (26 cycles) from –40° to 120°C had no effect on tensile and compressive stiffness, but shear modulus was reduced by 25%. Prior load cycling can substantially reduce Young's modulus. The fatigue limits presented in Section 4 were chosen, in part, to assure that the stiffness loss does not exceed 10%. Finally, long-term exposure (up to 5000 hours) in distilled water and 70% relative humidity (RH) and in windshield washer fluid (70% methanol/30% distilled water) led to stiffness reductions of at most 4%.

2.2 Creep Properties Long-term tensile creep tests were performed at room-temperature and at 70° and 120°C, as well as in distilled water and in windshield washer fluid. The latter tests (see Figure 2) were conducted after standard pre-exposures of 1000 hours in the case of distilled water and 100 hours in the case of windshield washer fluid.

The following empirical equation was developed for describing time-dependent creep strain at room temperature.

---

* At temperatures above 100°C and stresses greater than 140 MPa, the normally linear stress-strain response becomes slightly nonlinear, and this non-linearity is most pronounced at loading angles, like 22.5°, between fiber orientations.

$$\varepsilon_c = At^n \qquad [2]$$

where

$$A = 7.268 \times 10^{-10}\,\sigma^3 + 2.614 \times 10^{-8}\,\sigma^2 + 2.789 \times 10^{-5}\,\sigma + 2.960 \times 10^{-5}$$

$$n = 4.662 \times 10^{-7}\,\sigma^2 - 2.587 \times 10^{-4}\,\sigma + 0.2540\ .$$

The predictions of equation 1 are compared in Figure 3 with the results of several long-term creep tests. The agreement is good at the lower stresses. Localized damage accumulation at the higher stress levels led to increased data scatter, but on average, the agreement is reasonable.

The effect of increasing temperature on time-dependent creep strain can be accounted for by multiplying the strains predicted by equation 2 by a factor, which is plotted in Figure 4. For fluid effects, the results of tests performed under the two standard exposures, mentioned above, led to creep multiplication factors of 1.7 for distilled water and 1.5 for windshield washer fluid.

Creep under compressive stresses is much more matrix-dominated, and, at least at higher temperatures and stress levels, is likely to involve some local buckling. Limited compressive creep data indicate that at room temperature, compressive creep is the same as tensile creep. However, at 120°C, compressive creep appears to be much larger than tensile creep, and the factor, rather than being constant as in the tensile case, depends on stress level. Factors as high as 77 times the room-temperature tensile creep were found. Clearly long-term compressive loadings should be avoided at 120°C.

3. ALLOWABLE STRESSES FOR STATIC LOADINGS

The basic allowable stresses used in this section are time-dependent. They are derived from both instantaneous and creep-rupture tests. The system of allowable stresses used here follows that developed earlier for random-glass-fiber composites (4).

3.1 Short-Time Allowable Tensile Stress, S_0 The basic short-time, or instantaneous, allowable stress is based on the minimum room-temperature ultimate tensile strength (UTS), which is defined as the "B-basic stress" (5). The minimum room-temperature value is based on statistical treatment of n = 86 UTS values, such that the survival probability at the minimum stress is 90% at a confidence level of 95%. This minimum value was calculated to be 291 MPa. The allowable stress, S_0, is defined as two-thirds UTS_{min}. At room-temperature, S_0 thus becomes 194 MPa, which is 58% of the average UTS. Values of S_0 at other than room temperature were obtained by multiplying the room-temperature value by the ratio of the average at-temperature UTS to the room-temperature UTS.

The UTS, and hence S_0, can be reduced by several other effects. First a sequence of prior loading/unloading steps to 20%, 40%, 60%, and 80% of the average UTS was found to reduce

the subsequent UTS by 15%. While 80% UTS is significantly above S_0, a single prior loading to 80% UTS alone reduced the subsequent UTS by just 6%, so the lower stresses had a major effect. Thus, prior load effects should at least be considered in design. Second, prior thermal cycling between –40°C and 120°C reduced the subsequent UTS by almost 7%. Finally, while the standard fluid exposures did not reduce the UTS, exposure to humid air (70% RH) did. A reduction of almost 6% bounds the latter effect for exposure times up to almost 5000 hours. If all these reductions were applied simultaneously, the assumed effect on S_0 would be

$$S_0 = (0.85)\ (0.93)\ (0.94)\ 194 = 144 \text{ MPa}$$

Ultimately the designer must judge which factors are appropriate for the application.

3.2 Time-Dependent Allowable Tensile Stress, S_t For sustained loadings, creep-rupture stress is the basis for time-dependent allowable stresses, provided that S_0 is not lower than the creep-derived values. For uniaxial tension the time-dependent allowable stress, S_t, is defined as

$$S_t \leq \begin{cases} S_0 \\ 0.8\, S_r \end{cases} \qquad [3]$$

where S_r is the minimum creep-rupture strength. Note that S_t=S_0 at zero time.

The creep-rupture curves from which S_r was determined are shown in Figure 5. Because of the paucity of failure data, the "minimum" curves were established by simply shifting the original average curves down to bound all of the data points.

The Manson-Haferd time-temperature parameter was used to generate S_r values at other than room temperature and 120°C. Details of the use of the Manson-Haferd parameter can be found in reference (6). The parameter is expressed as

$$P_{MH}(\sigma) = \frac{T - T_a}{\log_{10} t_r - \log_{10} t_a} \qquad [4]$$

where T is temperature in degrees Rankin, and t_r is rupture time in hours. The constants T_a and t_a are determined by the interaction point of lines representing the available data at various stress levels on a plot of T vs $\log_{10} t_r$. The solid line in Figure 6 shows the resulting plot of tensile stress vs the Manson-Haferd parameter. Note that in this plot T is in °C. Creep-rupture stresses for various times at several specific temperatures were determined from the master curve and used, in turn, to determine reduction ratios of the stresses at each temperature relative to those at room temperature.

Values of S_t without environmental or prior load effects are plotted in Figure 7(a), where both S_0 and 0.8 S_r are shown. Only at the longer times and higher temperatures do the 0.8 S_r values drop below S_0. Figure 7(b) includes the effects of moisture/fluids on the allowables. The short-time S_0 value includes the 6% reduction due to exposure in a 70% RH air environment. For creep-rupture, curves similar to those in Figure 5 were developed for the two standard fluid exposures. Windshield washer fluid had the greatest effect; reductions ranged from 3% at 10 hours to 6% at 131,000 h (15 years). These reductions are included in the 0.8 S_r curves.

3.3 Compressive and Biaxial Allowable Stress, S_t^* To this point, the allowable stresses are based on, and thus only apply to, uniaxial tensile stress states. In design, where other stress states will likely exist, a simple biaxial strength criterion is needed. Because the current composite is isotropic in the plane of the material, a simple criterion is possible.

The available average strength data at room-temperature, though limited, are plotted in principal stress space in Figure 8, where they are compared with common biaxial strength theories. The solid points in the figure are from the basic tensile, compressive, and shear test results. The open-point compressive strength values come from tests of a "compression-after-impact" type specimen, which has antibuckling face-support plates. It is believed that the open points are a more accurate representation of the true compressive strength. Nonetheless, it was conservative to use the solid compressive and shear points, even though both may reflect the influence of buckling of the thin specimens. The tensile and open compression points are consistent with any of the criteria. However, the solid compression and shear points would dictate that the maximum shear theory is the best choice. Thus, it was adopted for evaluation of nontensile stress states.

Because temperature has essentially the same relative effect on both compressive and shear strengths, the maximum shear theory should be applicable at any temperature. Furthermore, fluids have a larger effect on compressive strength than on shear strength, so the maximum shear theory with the stress limited to the compressive strength, reduced by fluid effects, is conservative. For creep rupture, there are no available shear results, so the assumption must be made that the compressive results with the maximum shear strength criterion are still adequate.

Only two compressive creep-rupture test results, both at 120°C, were available. To estimate a full set of creep-rupture results, use was again made of the Manson-Haferd parameter. It was assumed that the tensile parameter also applies to compressive creep rupture, and the two compressive data points were plotted on Figure 6. The master curve shown for compression in Figure 6 has a much more tenuous basis than that for tension. In addition to assuming that the tensile constants are applicable to compression, it was assumed that the two master curves would be roughly parallel and that at large negative values of P_{MH}, the stress is limited by the ultimate compressive strength at room temperature – 225 MPa. With these assumptions, the curve was drawn.

The resulting allowable S_t^* stresses, without environmental or prior load effects, are plotted in Figure 9(a). Figure 9(b) depicts the values with estimated fluid effects included. Recall that an exposure to 70% RH air had the greatest impact on tensile strength – a reduction of 6%. That condition was not evaluated for compression, but of the two standard fluid exposures – distilled water and windshield washer fluid – distilled water had the greatest effect, and the reduction factor was also 6%. This reduction is the basis for the S_0^* curve in Figure 9(b). No compressive creep-rupture tests in fluids were performed, so the reduction factors used for tension were also used for the $0.8S_r^*$ values in Figure 9(b). Note that S^* is lower than the tensile allowable stress.

3.4 Treatment of membrane and Bending Stresses The S_t and S_t^* values establish limits on allowable in-plane membrane stresses, *P*. For out-of-plane bending away from structural discontinuities, the combined membrane plus bending stresses, $P + Q$, are limited to

$$P + Q \leq KS_t \left(or\ S_t^* \right) \qquad [5]$$

where K is 1.5 at –40° and 23°C, 1.3 at 70°C, and 0.9 at 120°C. These factors were derived from short-time beam flexure test results. It should be emphasized that equation 5 applies to bending stresses elastically calculated assuming an isotropic, homogeneous material. Also equation 5 does not apply to locations with geometric discontinuities (e.g., corners and bends). At such locations new failure modes can occur.

4. LIMITS FOR CYCLIC LOADINGS

Several series of fatigue tests were performed to provide a basis for design rules. Most of the tests were tension-tension fatigue, having a ratio, R, of minimum to maximum cyclic stress of 0.1. These tension-tension tests were used to generate S – N (stress vs cycles to failure) curves at various temperatures and for specimens exposed to the reference fluids.

In addition to the R = 0.1 tension-tension tests, mean stress tests involving four different cycle types were performed in air at room temperature. The cycle types were:

- R = 0 tension (zero to maximum stress),
- R = -∞ compression (zero to maximum compressive stress),
- R = -1 completely revered tension/compression, and
- tensile tests with a mean stress equal to 50% of the UTS.

While the standard dogbone-shaped tensile specimen was used for the R = 0.1 tensile tests, an hourglass-shaped specimen was used for the mean stress tests to minimize buckling under compressive loading.

4.1 Basic Fatigue Design Curves Two room-temperature, ambient-air design fatigue curves are provided. The first applies to cycles in which the stress varies from zero to a maximum tensile value (R = 0). The second curve applies to fully reversed cycles (R = -1), where the stress varies from a tensile stress to an equal, but opposite, compressive stress. This latter curve may be used with the Goodman relation to determine the allowable lives for cycles with other tensile or compressive mean stress values.

The tensile design curve, and its basis, is shown in Figure 10. Although the curve is intended to apply to R = 0 cycles, it is actually derived from R = 0.1 tensile cycling data. Comparative tests show that there is little difference in results from the two cycle types.* Two margins were used to derive the design curve. First, a margin of 20 was placed on cycles to failure. This assures that loss of stiffness, which was monitored during each fatigue test, does not exceed 10%. Second, an additional multiplication factor of UTS_{min}/UTS_{avg} = 0.90 was applied to stress to obtain the final design curve. This latter factor was judged to be necessary because of the significant scatter in fatigue life.

* R = 0.1 is used simply to avoid the risk of subjecting the slender tensile fatigue specimen to a compressive loading.

The second design curve, based on fully reversed (R = -1) cycling data, is provided in Figure 11. This second curve was developed by applying the same two design factors as used in the previous paragraph for tensile cycling.

Owen and Smith (7) suggested several forms of the Goodman relation for correlating composite fatigue results from tests with various mean stresses. The original basic form was found to work well for the quasi-isotropic composite.

$$S_a = S_e\left(1 - \frac{\sigma_m}{UTS}\right) \qquad [6]$$

Here, S_a is the alternating stress in a cycle having mean stress σ_m, and S_e is the alternating stress in a fully-reversed cycle (R = -1) at a given cyclic life (i.e., the predicted value of S_a is for the same cyclic life as that corresponding to S_e in the fully-reversed cycle). Using equation 6 with S_e determined from the data curve in Figure 11, it was possible to predict the S – N curve for each of the other three mean-stress cycle types, i.e., R = 0 tension, 50% UTS mean stress tension, and R = -∞ compression (the absolute value of the negative mean stress was used in this latter case). With the exception of the R = 0 tension case, where the prediction was somewhat conservative at the higher cycles, the agreement between measured and predicted fatigue lives was good. Thus, use of equation 6 and Figure 11 is recommended for assessing all design cycles except zero to tension loadings, in which case Figure 10 should be used.

4.2 Effects of Temperature and Fluids In addition to the tensile fatigue curve generated at room temperature, tensile curves were also developed for –40°, 70°, and 120°C. The fatigue strength multiplication factors given in Table 1 relate the strength at the various temperatures to the corresponding room-temperature strength. These factors are intended to be used with the design fatigue curves in Figures 10 and 11 to obtain design allowable cyclic stresses at other temperatures.

Table 1. Fatigue strength factors to account for temperatures

Temperature	Cycles			
(°C)	10^2	10^4	10^6	10^8
-40	0.89	1.03	0.96	0.88
23	1.00	1.00	1.00	1.00
70	1.00	0.97	0.89	0.82
120	0.97	0.78	0.62	0.50

Tensile fatigue curves were also generated for the two standard fluid exposures – testing in distilled water following a 1000 hour presoak, and testing in windshield washer fluid following a 100 hour presoak. Fatigue strength factors similar to those above were developed and are listed in Table 2. Again, these factors are intended to be used with the design fatigue curves in Figures 10 and 11.

Table 2. Fatigue strength factors for two bounding fluid environments

Environment	Cycles			
	10^2	10^4	10^6	10^8
Water, 1000 hour presoak	0.92	0.91	0.97	1.00
Windshield washer fluid, 100 hour presoak	0.97	0.92	0.95	0.98

5. SUMMARY

A tentative set of durability-based design criteria has been presented for a quasi-isotropic carbon-fiber composite for possible automotive structural application. The study was guided by 1) the need to establish criteria that could be readily integrated into the existing automotive structural design process and 2) the fact that it was not feasible to experimentally examine all possible combinations and conditions. Thus, simplifications, assumptions, and extrapolations were necessary, as is often the case when definitive design guidance must be provided.

The resulting criteria are summarized in Table 3 for key conditions. The allowable stresses in the table are expressed as a percentage of the average room-temperature UTS of 336 MPa.

Table 3. Key allowable stresses, expressed as a percentage of average room-temperature UTS

Stress allowable	Without fluid effects		With fluid effects	
	23°C	120°C	23°C	120°C
S_0	58	47	54	44
S_0^*	39	23	36	21
S_t				
5000 hours	58	42	54	40
15 yr	58	—[a]	54	—
S_t^*				
5000 hours	39	5	36	5
15 yr	39	—	36	—
S_{max} (R = 0)				
10^2 cycles	79	77	73	71
10^8 cycles	47	24	46	23

[a]Unrealistic condition

A strain limit of 0.3 to 0.4% has often been used, at least for glass-fiber composites, for design of composite automotive structures. The strain limit is intended to cover all effects. Strains of 0.3 and 0.4% correspond to 29% and 39% of the average room-temperature UTS, respectively. Comparison of these stress levels with the allowable values in Table 3 shows that the strain limits cover all the realistic tensile stress conditions except high-cycle fatigue at 120°C. The compressive and biaxial allowables at 120°C would not be met.

The strain limits are overly conservative in large regions of Table 3. The limits given in this paper put the design allowables on a more rational and defensible basis and avoid the over- and underconservatism associated with the simplified strain limit approach.

6. REFERENCES

1. J.M. Corum, et al., Durability-Based Design Properties of Reference Crossply Carbon-Fiber Composite, ORNL/TM 2000/322, Oak Ridge National Laboratory, Oak Ridge, Tennessee, April 2001.
2. J.M. Corum, et al., Durability-Based Design Criteria for a Quasi-Isotropic Carbon-Fiber Automotive Composite, ORNL/TM-2002/39, Oak Ridge National Laboratory, Oak Ridge, Tennessee, March 2002.
3. J.M. Corum, et al., Recommended Minimum Test Requirements and Test Methods for Assessing Durability of Random-Glass-Fiber Composites, ORNL-6953, Oak Ridge National Laboratory, Oak Ridge, Tennessee, June 1999.
4. J.M. Corum, et al., Composites Science and Technology, **61**, 1083 (2001).
5. The Composite Materials Handbook – MIL 17, **I**, Guidelines for Characterization of Structural Materials, Revision MIL-HDBK-17-1E, Technomic Publishing Co., Inc., Lancaster, Pennsylvania, January 1997.
6. H. Kraus, Creep Analysis, John Wiley and Sons, New York, 1980, pp. 103-104.
7. M.J. Owen and T.R. Smith, Plastics and Polymers, 33 (February 1968).

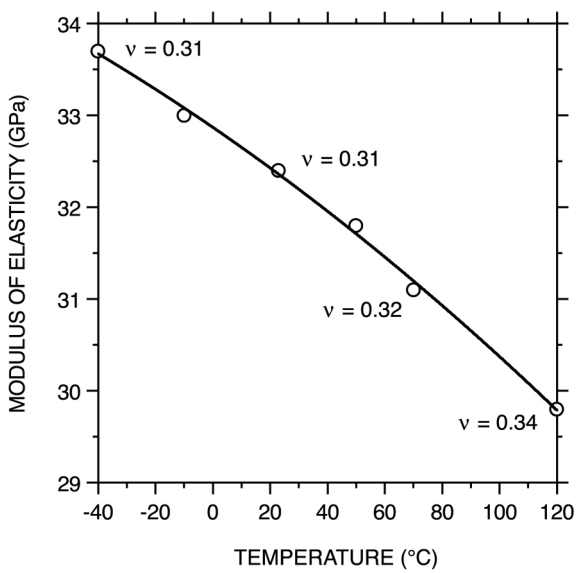

Figure 1. Variation of elastic modulus with temperature. Poisson's ratio values are shown at specific temperatures.

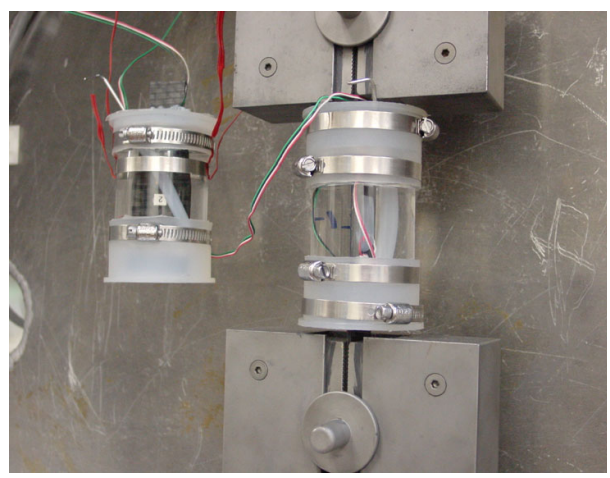

Figure 2. Creep specimen submerged in fluid under load. An unstressed piece of material with dummy strain gages, used for full-bridge compensation, is in the second container. This compensation was used for all creep tests.

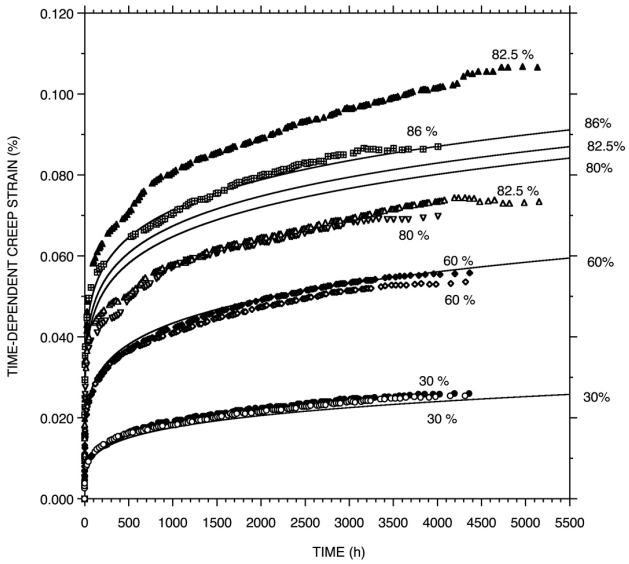

Figure 3. Measured and predicted time-dependent creep strains at room temperature. Stress levels are expressed as a percentage of the UTS of 336 MPa.

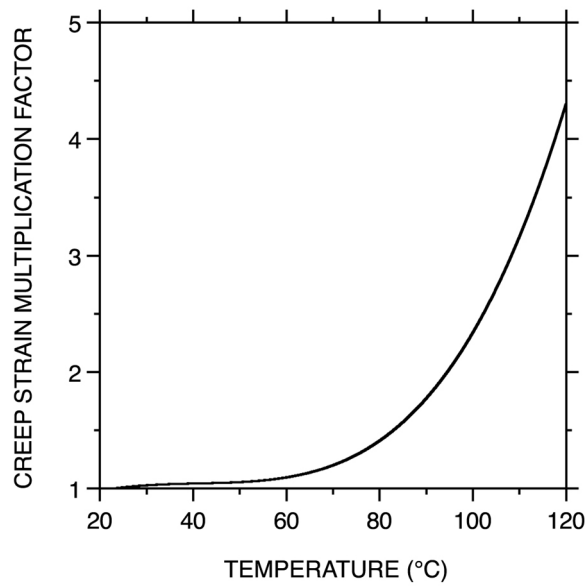

Figure 4. Factor for determining creep at various temperatures from room-temperature curves.

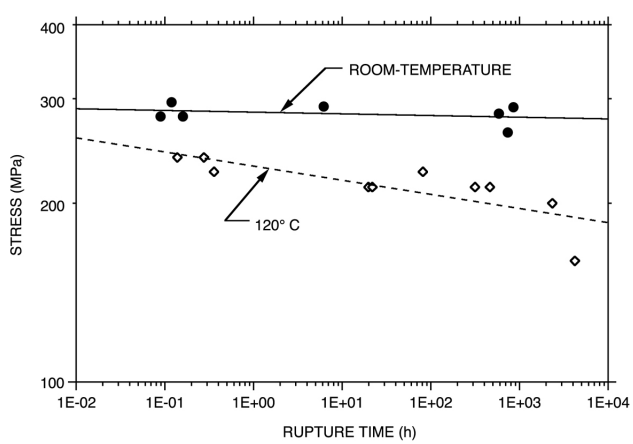

Figure 5. Creep-rupture curves at room-temperature and 120°C.

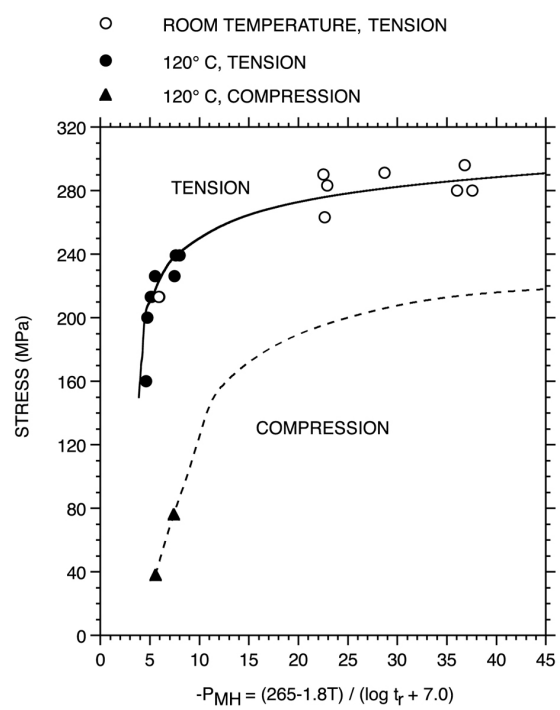

Figure 6. Manson-Haferd parameter curves for tension and compression.

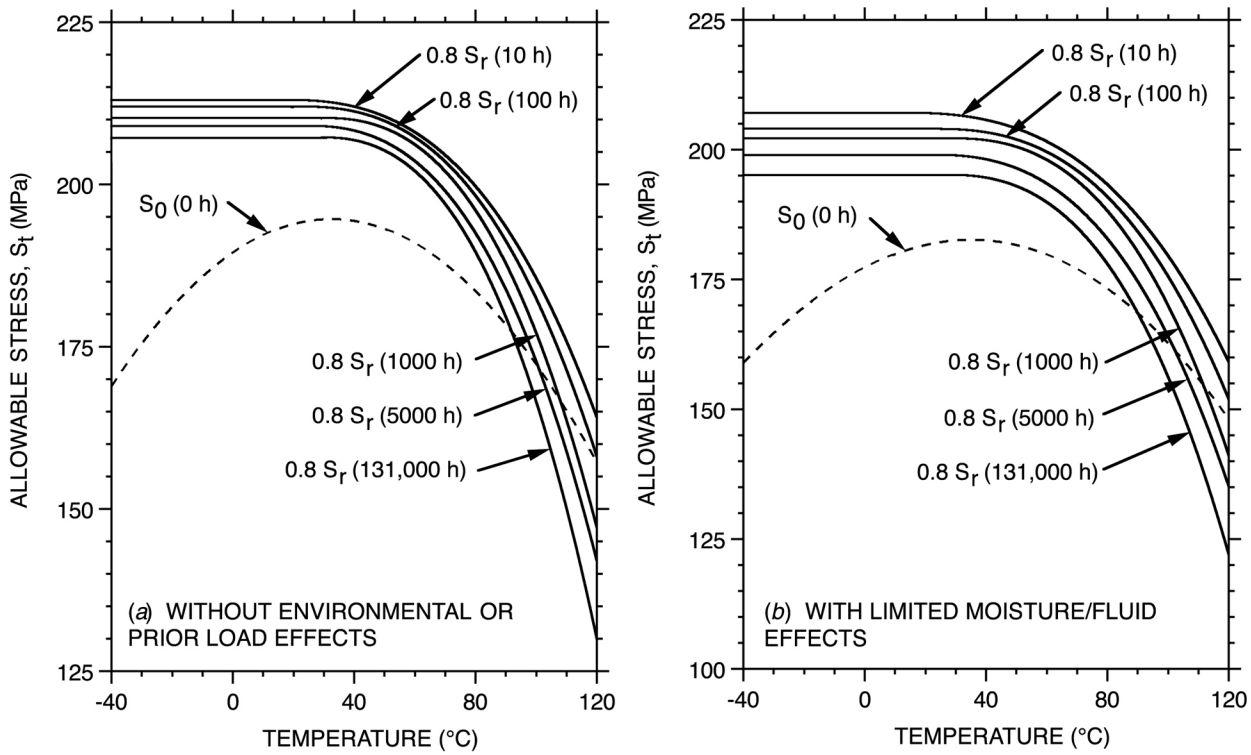

Figure 7. Allowable tensile stresses, S_t. Note that S_t is the lower of S_0 and 0.8 S_r.

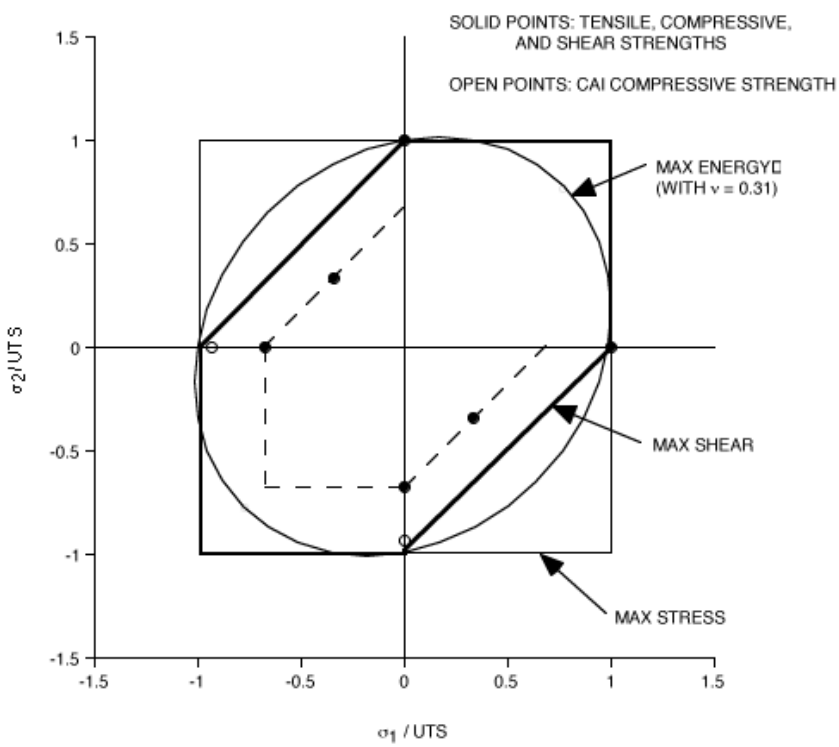

Figure 8. Candidate failure criteria compared with available room-temperature failure data. Stresses are shown as a fraction of the UTS of 336 MPa.

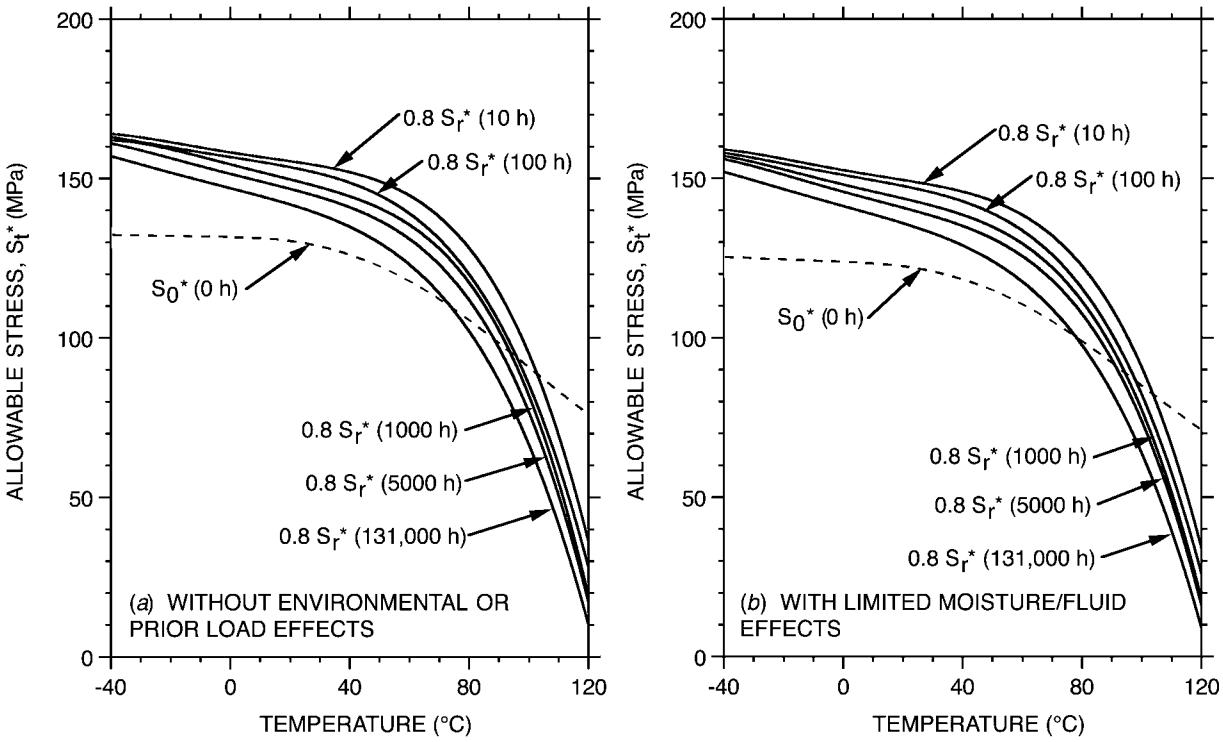

Figure 9. Allowable compressive and nontensile biaxial stresses, S_t^*.

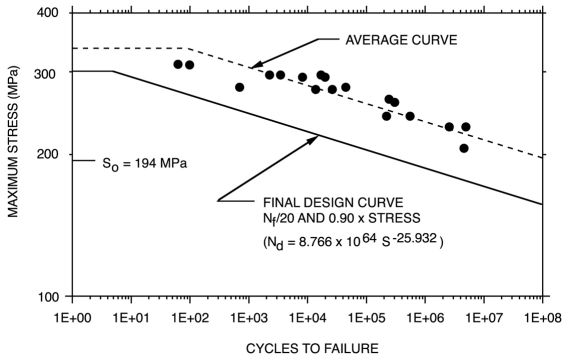

Figure 10. Derivation of room-temperature design fatigue curve for tensile cycling.

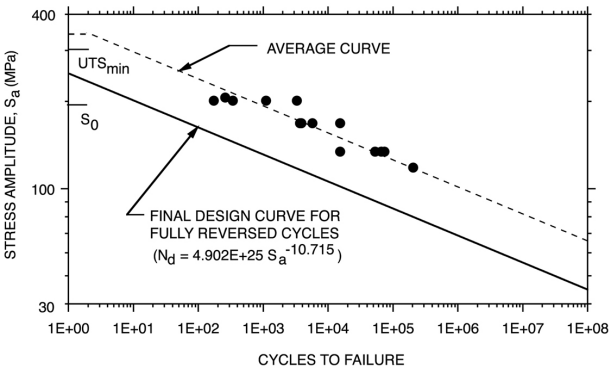

Figure 11. Room-temperature design fatigue curve for fully-reversed cycling.